

# Field Strength Simulation of Typical Defects in XLPE Cable

Lei Tao

*School of Electrical and Control Engineering, Heilongjiang University of Science and Technology, Harbin, Heilongjiang, 150022, China*

**Abstract:** *Crosslinked polyethylene (XLPE) cables are now widely used in power transmission. Due to various factors, XLPE cables are unavoidable to produce defects during installation, transportation and use. These defects can easily cause partial discharge and even lead to cable breakdown accidents, which can cause great losses.<sup>[1]</sup> In this paper, three typical defects in XLPE cables are studied: air gap defect inside XLPE insulation, metal spike defect on the surface of insulation layer and metal particle defect on the main insulation surface. Electric field simulation is carried out by COMSOL finite element software. Three corresponding cable models under 132kV DC voltage are established, and the simulation analysis of electric field strength is carried out. The field strength distributions for different defects are obtained. The results show that the overall electric field strength of the insulation defect decreases with the distance from the surface of the cable insulation layer. However, the distortion of the electric field strength at the defect is different according to the location and size of the insulation defect. It needs to be simulated under different conditions.*

**Keywords:** *Crosslinked polyethylene cable, typical defect, Finite element software, electric field strength, Partial discharge, Electric field distortion*

## 1. Introduction

Cross linked polyethylene (XLPE) cable has superior electrical performance. It is easy to lay and has large transmission capacity<sup>[2][3]</sup>. Compared with other materials, XLPE cable has smaller diameter, lighter weight and simple accessory joint. Therefore, XLPE cable is widely used in power supply network. However, cables often encounter some unavoidable damages in the process of production, transportation, installation and operation<sup>[4]</sup>; At the same time, in the process of cable use, it is also easy to be affected by other external factors such as humidity, temperature, light, chemical substances and machinery in the external environment<sup>[5]</sup>. This series of factors lead to cable insulation defects. Typical defects in XLPE cable include: air gap defect inside the insulating layer, metal spike defect and metal particle defect attached to the main insulation of the cable. These insulation defects are easy to induce partial discharge during long-term operation under high field strength<sup>[6][7]</sup>. Long-term partial discharge will not only aging the cable, affect the insulation life of the cable and cause accidents.

HVDC transmission technology is an important development trend of today's transmission technology. Although the research on XLPE cable in China started late, XLPE cable has developed rapidly under the background of West to East power transmission and the construction of the Middle East since the 1970s, and has a good application prospect<sup>[8]</sup>. Taking the concentric shaft 132kV XLPE cable as the model, the cable model is built in COMSOL finite element simulation software to simulate and study the electric field distribution. The software can not only visually see the distribution of electric field intensity in the cable, but also show the distribution of different electric field intensity in the case of different defects in the cable<sup>[9]</sup>. The study of electric field intensity distribution under typical defects in XLPE cable has important practical reference value to ensure the stability of cable operation and power supply reliability.

## 2. Establishment of Cable Defect Model

### 2.1. XLPE Cable Model

The steady-state field strength distribution is obtained by simulating the electric field strength in the electrostatic field. The characteristics of the electric field strength distribution are studied when different

defects occur in the XLPE cable. The equations for calculating the electrostatic field are as follows:

$$\nabla \cdot D = \rho v \quad (1)$$

$$E = -\nabla V \quad (2)$$

In order to save simulation time, a simulation model of two-dimensional coaxial crosslinked polyethylene cable is built, as shown in Fig. 1.

Single-core cross-linked polyethylene direct current cable is generally extruded by 9-layer structure including conductor shield layer, XLPE insulation layer, insulation shield layer 3, and conductor core, conductor envelope, semi-conductive water resistance zone, wrinkle aluminium sheath, anti-corrosion layer and outer sheath. The simulation model is based on these nine layers, as shown in Figure 1. The material, relative dielectric constant and outer diameter of each layer are shown in Table 1.

*Table 1: Cable structure material and outer diameter.*

structure	Material	Relative dielectric constant	external diameter (mm)
Conductive core	copper	10000	16.0
Conductor tape	nylon	100	16.6
Conductor shielding	XLPE	2.3	19.1
Insulation layer	XLPE	2.3	57
Insulation shielding	XLPE	2.3	59.3
Semiconductive Waterband	silicon	100	64
corrugated aluminium sheath	aluminium	1	76.5
Anti-Corrosion Layer	asphalt	4	78.5
sheath	polyvinyl chloride	3	86.5

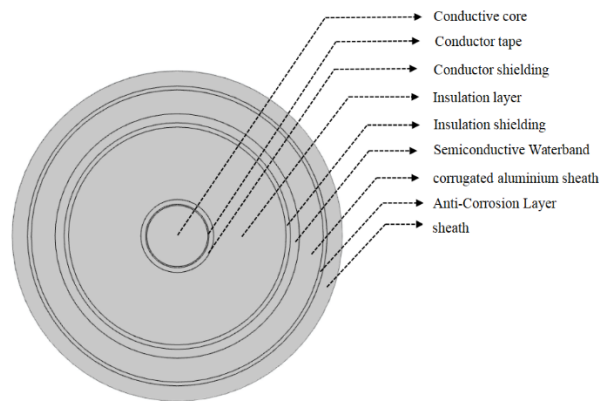


*Figure 1: Diagram of XLPE cable layer structure.*

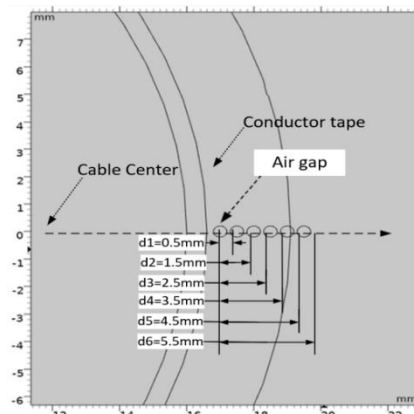


*Figure 2: Air gap defect simulation model.*

During the production, installation and operation of XLPE cable, various insulation defects will occur due to factors such as inadequate cable extrusion during production or construction errors when stripping the semi-conductive layer outside the insulating layer. Common defects in engineering include: air gap defects in the insulating layer, metal spikes on the surface of the insulating layer, metal particles attached to the main insulating surface. In this paper, the model will be established around these three defects, the

electric field strength will be simulated and analyzed.

## 2.2. Air Gap Defects

When making XLPE cable insulation layer, because the cable conductor is damp or the cross-linking by-product impurities are generated, bubbles will remain in the insulation layer in the insulation extrusion link, which is called a typical "air gap defect". The established simulation model is shown in Figure 2 above. The diameter of this bubble defect is generally about a few microns to hundreds of microns. In order to facilitate simulation observation, the bubble model is set as a circle with a radius of 0.2mm. By constantly adjusting the location and size of bubble defects, the influence of bubble location and size on cable electric field strength is observed according to the corresponding electric field strength distribution.

## 2.3. Prick Defect

In the process of XLPE cable installation or operation, due to the influence of process level, there will be impurities in the cable layer or tip protrusion in the outer semiconducting layer of the cable, which is called typical "metal spike defect". The simulation model is shown in Figure 3. In this defect, the simulated steel needle prick model is radially inserted into the central insulating layer of the cable and does not contact the wire core; The length is 6.8cm, the width is 2cm, the radius of curvature of the needle is about  $5\ \mu\text{m}$  and the angle of the needle tip is  $30^\circ$ . Such defects are easy to produce electrical branches and lead to partial discharge. Long term partial discharge may cause cable insulation breakdown and cause harm.

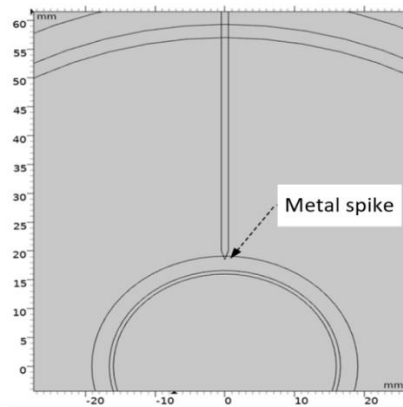


Figure 3: Prick defect simulation model.

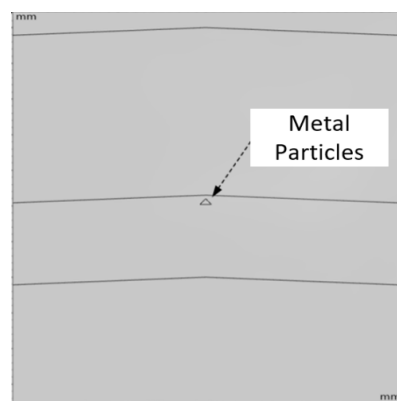


Figure 4: Metal particle defect simulation model.

## 2.4. Metal Particle Defect

In the production process of XLPE cable, sometimes due to the mistakes of workers, impurities such as metal particles will be attached to the main insulation surface of the cable and close to the outer semiconducting layer, which is called "metal particle defect". Its simulation model is shown in Figure 4. In this defect, the metal particle model has an area of  $0.026\text{mm}^2$ . The center point of each triangular

particle is vertical and orderly, and is arranged on a vertical line with the center of the cable circle. The material is common copper. With the different position, size and shape of metal particles, the corresponding electric field intensity distribution is also different.

### 3. Simulation Results and Analysis

Using the finite element software COMSOL for simulation solution, the electric field intensity distribution diagram of XLPE cable without defects is obtained, as shown in Figure 5. It can be clearly seen from the figure that the closer to the center of cable insulation layer, the greater the electric field intensity; According to the figure, the maximum electric field strength of conductor shielding layer is 4.5kv/mm, and the minimum electric field strength of conductive wire core, cladding layer and semi conductive resistance water belt layer is close to 0kv / mm.

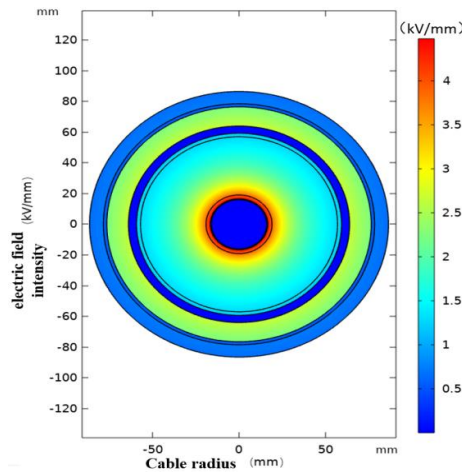


Figure 5: Electric field intensity of XLPE cable.

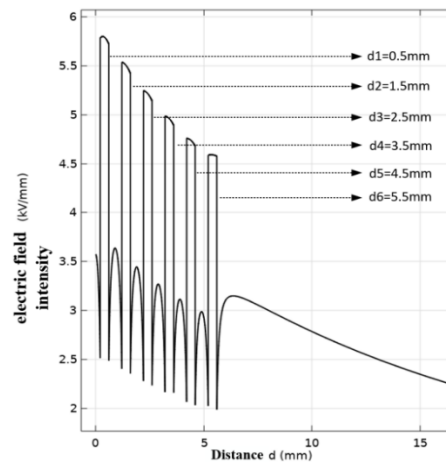


Figure 6: Electric field intensity of air gap defects at different positions.

#### 3.1. Electric Field Simulation of Air Gap Defects inside Cable Insulation

When the size of the air gap remains unchanged and the position of the air gap in the insulating layer is changed, a total of 6 air gap models are established, with a radius of 0.2mm. The distance from the position to the conductor cladding layer is  $d_1=0.5\text{mm}$ ,  $d_2=1.5\text{mm}$ ,  $d_3=2.5\text{mm}$ ,  $d_4=3.5\text{mm}$ ,  $d_5=4.5\text{mm}$ ,  $d_6=5.5\text{mm}$  respectively. A two-dimensional section line is made horizontally and vertically from the center of the air gap (through the three layers of insulation), The electric field intensity distribution and specific distortion with air gap defects are obtained after simulation, as shown in Figure 6.

It can be observed from Fig. 6 that at the air gap insulation, the electric field intensity is distorted. Firstly, through transverse observation, it can be observed that as the air gap is farther and farther away from the conductor cladding layer of the cable, the maximum electric field intensity at the defect also decreases, from the maximum electric field intensity  $E_{\text{max}1} = 5.81\text{kv/mm}$  when  $d_1 = 0.5\text{mm}$  to the

maximum electric field intensity  $E_{max5} = 4.59\text{kv/mm}$  when  $d_6 = 5.5\text{mm}$ ; At the same time, as the air gap is farther away from the center of the cable, the maximum electric field intensity at the air gap defect decreases and the speed decreases. Longitudinal observation shows that the electric field intensity at the defect with air gap is much larger than that without defect, and the electric field intensity at the defect with air gap first increases and then decreases rapidly, and the electric field intensity changes rapidly.

In order to make the simulation results more obvious, the position of the air gap is set to be  $d = 0.5\text{mm}$  from the conductor cladding layer, and the radii are  $r_1=0.05\text{mm}$ ,  $r_2=0.1\text{mm}$ ,  $r_3=0.2\text{mm}$ ,  $r_4=0.3\text{mm}$ ,  $r_5=0.4\text{mm}$  respectively. Take the center of the air gap as the starting point and make a two-dimensional section horizontally, the electric field intensity distribution and specific distortion with air gap defects after simulation are shown in Figure 7. It can be observed from Fig. 7 that the change of radius in air gap defect has no obvious effect on the electric field intensity. With the increase of the radius, the closer to the surface of the insulating layer, the electric field intensity at the defect decreases slowly; According to the electric field intensity at the radius, the electric field intensity at the defect decreases more and more with the decrease of the radius of the air gap;

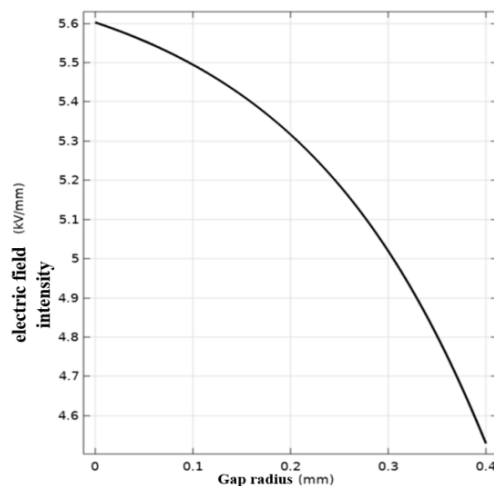


Figure 7: Electric field intensity of air gap defects.

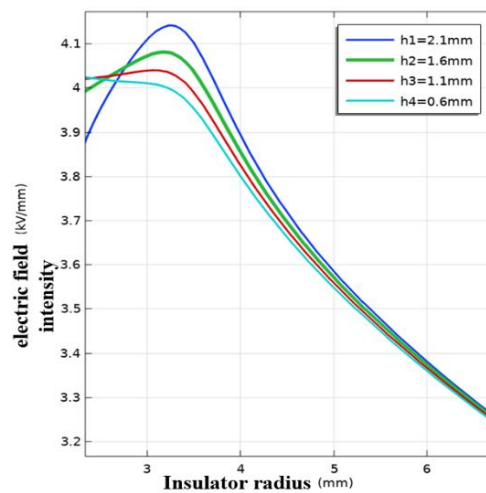


Figure 8: Electric field strength of metal spikes under different rad at different depths.

### 3.2. Electric Field Simulation of Metal Spike Defect on the surface of Insulating Layer

Keep other conditions unchanged and change the depth of the metal spike inserted into the conductor shielding layer. A total of four spike models are established. The depths are  $h_1=2.1\text{mm}$ ,  $h_2=1.6\text{mm}$ ,  $h_3=1.1\text{mm}$ ,  $h_4=0.6\text{mm}$  respectively. Take the cable center as the starting point and the needle tip penetrating the spike as the direction to make a two-dimensional section. The distribution of electric field intensity and distortion obtained by simulation are shown in Figure 8 below. From the analysis of a single curve, the electric field intensity at the tip of the needle shows an upward trend, and the electric field intensity is the largest. For example, when the spike is inserted into the insulating part of the cable is

2.1mm, the maximum electric field intensity of the tip is 4.14kv/mm, and then the electric field intensity decreases gradually.

From the comparison of the curves in Fig. 8, Distortion at the prick defect: observe the maximum value of electric field intensity, and it is found that the distortion at the needle tip of the prick is the most obvious, and the electric field intensity is also the largest, which is most prone to insulation breakdown. At the same time, by longitudinal comparison of multiple curves, it can be found that the deeper the metal spike is inserted into the insulating part of the cable, the greater the electric field intensity is obtained. This phenomenon is more likely to cause partial discharge.

### 3.3. Electric Field Simulation of Metal Particle Defect on Main Insulation Surface

Keep the size of the metal particles unchanged, change the position of the metal particles on the surface of the insulating layer, set the distance between the metal particles and the surface of the insulating layer as  $d_1=1\text{mm}$ ,  $d_2=2\text{mm}$ ,  $d_3=3\text{mm}$ ,  $d_4=4\text{mm}$ ,  $d_5=5\text{mm}$  respectively, and make a vertical two-dimensional section with the center of the cable as the starting point and the center point of each triangular metal particle as the direction, The distribution of electric field intensity at five different positions after simulation calculation is obtained, as shown in Fig. 9. Through the horizontal comparison in Fig. 9, it can be observed that the farther the metal particles are from the surface of the insulating layer, the electric field intensity also increases.

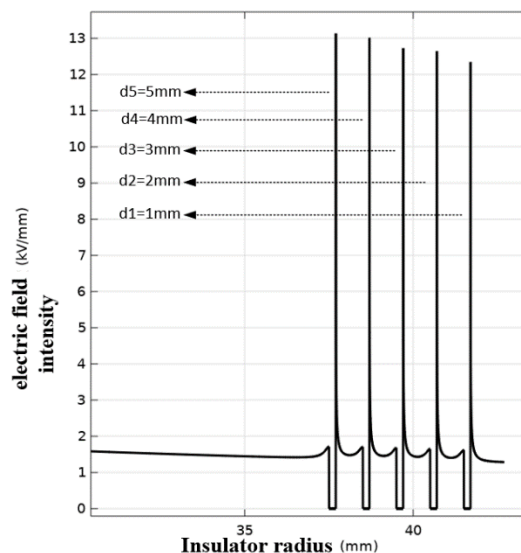


Figure 9: Electric field intensity of metal particles at different positions.

The maximum electric field intensity of metal particle defects under the condition of  $d_5=5\text{mm}$  can reach 13.12kv/mm, and the maximum electric field intensity of metal particles when  $d_1=1\text{mm}$  is only 12.33kv/mm. Through further observation, it can be found that the closer the metal particles are to the surface of the cable insulation layer, the smaller the reduction range of the maximum electric field intensity is, and the influence on the maximum electric field intensity is gradually reduced.

## 4. Conclusions

In order to explore the influence of typical defects in XLPE cable on the distribution of electric field intensity, COMSOL finite element software is used to simulate three typical insulation defects. By adjusting the location and size of defects and observing the corresponding electric field intensity distribution, the following conclusions can be obtained:

(1) When there is no defect, the electric field intensity distribution of XLPE cable is as follows: the closer it is to the surface of cable insulation layer, the lower the electric field intensity.

(2) When there are air gap defects in the cable insulation, the position of the air gap has a greater distortion on the electric field intensity than the radius. As the position of the air gap is closer to the surface of the cable insulation layer, the distortion at the defect decreases gradually, and the electric field intensity also decreases; When the radius increases, the range of distortion increases.

(3) When the metal spike defect exists, the deeper the spike is inserted into the insulating layer, the degree of distortion increases. At the same time, the distortion at the needle tip is the most serious, and the maximum electric field intensity reaches 4.14kV/mm, while the electric field intensity inside the spike is 0.

(4) The distortion degree of the metal particle defect near the surface of the cable insulation layer becomes weaker with the position closer to the surface of the cable insulation layer; At the same time, the distortion degree at the edge of metal particles is the largest.

## References

- [1] Shan Bingliang, Li Shuning, Yang Xiao, Wang Wei, Li Chengrong Key problems faced by XLPE distribution cable defect diagnosis and location technology [J]. 2021,36 (22): 4809-4819
- [2] Zhang Long, Zhang Wei, Li Ruipeng, Li Hongjie, Terminal defect simulation and electric field analysis of 10kV XLPE cable [J]. Insulating materials, 2014,47 (04): 83-88
- [3] Zhang Xuan, Wan Shuting, Liu Ronghai, Wu Zhangqin, Numerical analysis of electric field of cable main insulation defects [J]. Yunnan electric power technology, 2015,43 (03): 105-109
- [4] Zhao Peng, Design of HVDC XLPE cable accessories based on COMSOL simulation [D]. China Electric Power Research Institute, 2018.
- [5] Li Wenquan, Research on fault diagnosis and location of main insulation of high voltage XLPE cable [J]. Electrical switch, 2021,59 (01): 94-98.
- [6] Hu Kai, Lu Zhifei, Yang Fengyuan, Zhang Lei, Typical defect simulation, PD research of HVDC XLPE cable [C], 2018 excellent proceedings of Zhejiang electric power society, 2018: 324-331.
- [7] Du Hao, Guan Hong Lu, Chen Xiangrong, Hou Shuai, Partial discharge characteristics of typical defects of XLPE cable under DC voltage [J] High voltage technology, 2021, 47 (02): 555-563.
- [8] He Ruobing, Chen Jia, Zhu Jinsong, Yang Xu, Yao Yuhang, Pan Cheng, PD characteristics and type identification of typical insulation defects of AC XLPE cable [J]. Electrician, 2020 (06): 5-13.
- [9] Ma Xin, Zhang Huaiyin, Wu Jiyan, Tuo Ping, Effect of temperature on partial discharge characteristics of spiked defects in XLPE cables [J]. High voltage apparatus, 2021, 57 (05): 151-156